Journal of Physics: Conference Series **600** (2015) 012058 doi:10.1088/1742-6596/600/1/012058

# Comparison between the fCCZ4 and BSSN formulations of Einstein equations in spherical polar coordinates

**N. Sanchis-Gual[1], P. J. Montero[2], J. A. Font[1,3], E. Müller[2] and T. W. Baumgarte[4]**

[1]Departamento de Astronomía y Astrofísica, Universitat de València, Dr. Moliner 50, 46100, Burjassot (València), Spain.
[2]Max-Planck-Institut für Astrophysik, Karl-Schwarzschild-Str. 1, 85748, Garching bei München, Germany.
[3]Observatori Astronòmic, Universitat de València, C/ Catedrático José Beltrán 2, 46980, Paterna (València), Spain.
[4]Department of Physics and Astronomy, Bowdoin College, Brunswick, ME 04011, USA.

E-mail: nicolas.sanchis@uv.es

**Abstract.** Recently, we generalized a covariant and conformal version of the Z4 system of the Einstein equations using a reference metric approach, that we denote as fCCZ4. We successfully implemented and tested this approach in a 1D code that uses spherical coordinates and assumes spherical symmetry, obtaining from one to three orders of magnitude reduction of the Hamiltonian constraint violations with respect to the BSSN formulation in tests involving neutron star spacetimes. In this work, we show preliminary results obtained with the 3D implementation of the fCCZ4 formulation in a fully 3D code using spherical polar coordinates.

## 1. Introduction

The Z4 formulation [1] of the Einstein equations is an extension of these equations obtained by adding a four vector ${}^{(4)}Z_\mu$ to the original system. Given a set of initial data which are a solution of the original Einstein equations, the extended equations will yield the same solution provided that at the initial time slice ${}^{(4)}Z_\mu = 0$. Any deviation from the solution of the original Einstein equations will then propagate away. Two conformal and traceless decomposition of the Z4 system have been recently proposed, namely the Z4c formulation [2, 3, 4, 5] and the CCZ4 formulation [6, 7]. Both of them incorporate the constraint damping scheme developed by [8]. This scheme allows to control dynamically the constraint violations by means of constraint damping terms, which are parametrized by two constants $\kappa_1$ and $\kappa_2$. Both formulations have been extensively tested and results show a reduction of the Hamiltonian constraint violations from one to three orders of magnitude with respect to BSSN [9, 10, 11], the actual values depending on the particular tests considered.

In a recent paper [12] we proposed a generalized covariant and conformal version of the Z4 system of the Einstein equations by adopting a reference metric approach. This approach, which we call fCCZ4 for short, reduces to the CCZ4 formalism in Cartesian coordinates, but is well-suited for curvilinear coordinates as well. In [12] we implemented this fCCZ4 formalism in a 1D

code that employs spherical polar coordinates under the assumption of spherical symmetry using a partially-implicit Runge-Kutta (PIRK) method. This scheme sidesteps the use of traditional regularization procedures when using spherical coordinates and allowed us to evolve both vacuum and non-vacuum spacetimes in spherical symmetry without encountering numerical instabilities. We performed several tests and compared violations of the Hamiltonian constraint in the fCCZ4 with those in the BSSN systems for different choices of the free parameters $\kappa_1$ and $\kappa_2$. For an optimal choice of parameters and for neutron star spacetimes, the violations of the Hamiltonian constraint are between 1 and 3 orders of magnitude smaller in the fCCZ4 system than in the BSSN formulation. However, for black hole spacetimes the advantages of fCCZ4 over BSSN are less evident.

The next logical step in our program was to implement and test the fCCZ4 formulation in a fully 3D code. This has been accomplished recently and preliminary results are reported in this work. In our research we employ our 3D code `nada`, whose ability to accurately handle numerical evolutions using spherical polar coordinates without any symmetry assumption adopting a covariant form of the BSSN formulation was recently shown in [13] and more recently by [14] who reported the first successful implementation of relativistic hydrodynamics coupled to dynamical spacetimes in spherical polar coordinates with no symmetry assumptions. The new fCCZ4 formulation has been assessed and compared with BSSN by performing two tests in 3D. We anticipated to find the same trend already observed in the spherically symmetric case and that has been indeed the case; that is, we observe a reduction in the violation of the Hamiltonian constraint of several orders of magnitude for fCCZ4 with respect to BSSN also in 3D.

## 2. The Fully Covariant and Conformal Z4 Formulation

In the Z4 system, the Hamiltonian and momentum constraints result in equations for the four-vector ${}^{(4)}Z_\mu$. In a 3+1 decomposition, these equations can be written as evolution equations for the projection of the ${}^{(4)}Z_\mu$ along the normal $n^\mu$, which, following standard convention, we define as $\Theta \equiv -n_\mu {}^{(4)}Z^\mu = \alpha\, {}^{(4)}Z^0$, and the spatial projection of ${}^{(4)}Z_\mu$, $Z_i \equiv \gamma_i{}^{\mu (4)}Z_\mu$. Here $Z_i$ denotes a spatial vector whose index can be raised with the (inverse) spatial metric, $Z^i = \gamma^{ij} Z_j$.

By defining

$$\partial_\perp \equiv \partial_t - \mathcal{L}_\beta \tag{1}$$

where $\mathcal{L}_\beta$ denotes the Lie derivative along the shift vector $\beta^i$, the fully covariant and conformal Z4 system in a reference-metric approach (fCCZ4) is then given by the following set of evolution equations:

$$\partial_\perp \bar\gamma_{ij} = -\frac{2}{3}\bar\gamma_{ij}\bar D_k\beta^k - 2\alpha\bar A_{ij}, \tag{2}$$

$$\begin{aligned}\partial_\perp \bar A_{ij} = &-\frac{2}{3}\bar A_{ij}\bar D_k\beta^k - 2\alpha\bar A_{ik}\bar A^k_j + \alpha\bar A_{ij}(K-2\Theta) + e^{-4\phi}[-2\alpha\bar D_i\bar D_j\phi \\ &+4\alpha\bar D_i\phi\bar D_j\phi + 4\bar D_{(i}\alpha\bar D_{j)}\phi - \bar D_i\bar D_j\alpha + \alpha(\bar R_{ij} + D_iZ_j + D_jZ_i - 8\pi S_{ij})]^{\rm TF},\end{aligned} \tag{3}$$

$$\partial_\perp \phi = \frac{1}{6}\bar D_i\beta^i - \frac{1}{6}\alpha K, \tag{4}$$

$$\begin{aligned}\partial_\perp K = &\, e^{-4\phi}[\alpha(\bar R - 8\bar D^i\phi\bar D_i\phi - 8\bar D^2\phi) - (2\bar D^i\alpha\bar D_i\phi + \bar D^2\alpha)] + \alpha(K^2 - 2\Theta K) + 2\alpha D_iZ^i \\ &-3\alpha\kappa_1(1+\kappa_2)\Theta + 4\pi\alpha(S-3E),\end{aligned} \tag{5}$$

$$\begin{aligned}\partial_\perp \Theta = &\, \frac{1}{2}\alpha[e^{-4\phi}(\bar R - 8\bar D^i\phi\bar D_i\phi - 8\bar D^2\phi) - \bar A^{ij}\bar A_{ij} + \frac{2}{3}K^2 - 2\Theta K + 2D_iZ^i] - Z^i\partial_i\alpha \\ &-\alpha\kappa_1(2+\kappa_2)\Theta - 8\pi\alpha E,\end{aligned} \tag{6}$$

$$\partial_\perp \tilde\Lambda^i = \bar\gamma^{jk}\hat D_j\hat D_k\beta^i + \frac{2}{3}\Delta\Gamma^i\bar D_j\beta^j + \frac{1}{3}\bar D^i\bar D_j\beta^j - 2\bar A^{jk}(\delta^i{}_j\partial_k\alpha - 6\alpha\delta^i{}_j\partial_k\phi - \alpha\Delta\Gamma^i_{jk})$$

$$-\frac{4}{3}\alpha\bar{\gamma}^{ij}\partial_j K + 2\bar{\gamma}^{ki}(\alpha\partial_k\Theta - \Theta\partial_k\alpha - \frac{2}{3}\alpha K Z_k) - 2\alpha\kappa_1\bar{\gamma}^{ij}Z_j - 16\pi\alpha\bar{\gamma}^{ij}S_j. \quad (7)$$

Here the superscript TF denotes the trace-free part of a tensor, $\kappa_1$ and $\kappa_2$ are the damping coefficients introduced by [8], and $\hat{D}_i$, $D_i$ and $\bar{D}_i$ denote the covariant derivatives built from the connection associated with the reference metric $\hat{\gamma}_{ij}$, the physical metric $\gamma_{ij}$ and the conformal metric $\bar{\gamma}_{ij}$, respectively. We have also defined

$$\tilde{\Lambda}^i \equiv \Delta\Gamma^i + 2\bar{\gamma}^{ij}Z_j, \quad (8)$$

where

$$\Delta\Gamma^i = \bar{\gamma}^{jk}\Delta\Gamma^i_{jk}. \quad (9)$$

The vector $\tilde{\Lambda}^i$ plays the role of the "conformal connection functions" in the original CCZ4 system; its evolution equation (7) involves the evolution equation for the variables $Z_i$.

The matter sources $E$, $S_i$, $S_{ij}$ and $S$ denote the density, momentum density, stress, and the trace of the stress as observed by a normal observer, respectively:

$$E \equiv n_\mu n_\nu T^{\mu\nu}, \quad (10)$$
$$S_i \equiv -\gamma_{i\mu}n_\nu T^{\mu\nu}, \quad (11)$$
$$S_{ij} \equiv \gamma_{i\mu}\gamma_{j\nu}T^{\mu\nu}, \quad (12)$$
$$S \equiv \gamma^{ij}S_{ij}. \quad (13)$$

In Eq. (3), we compute the Ricci tensor $\bar{R}_{ij}$ associated with $\bar{\gamma}_{ij}$ from

$$\bar{R}_{ij} = -\frac{1}{2}\bar{\gamma}^{kl}\hat{D}_k\hat{D}_l\bar{\gamma}_{ij} + \bar{\gamma}_{(i}\hat{D}_{j)}\Delta\Gamma^k + \Delta\Gamma^k\Delta\Gamma_{(ij)k} + \bar{\gamma}^{kl}(2\Delta\Gamma^m_{k(i)}\Delta\Gamma_{j)ml} + \Delta\Gamma^m_{ik}\Delta\Gamma_{mjl}). \quad (14)$$

Here we compute the $\Delta\Gamma^i$ from their definition (9). Given $\Delta\Gamma^i$, and values for $\tilde{\Lambda}^i$, the vectors $Z_i$, which are not evolved independently, can be determined from (8).

Unless stated otherwise we fix the gauge freedom by imposing the so-called "non-advective 1+log" condition for the lapse

$$\partial_t\alpha = -2\alpha(K - 2\Theta), \quad (15)$$

and a variation of the "Gamma-driver" condition for the shift vector

$$\partial_t\beta = B^i, \quad (16)$$
$$\partial_t B^i = \frac{3}{4}\partial_t\tilde{\Lambda}^i. \quad (17)$$

Finally, when $\Theta = Z_i = 0$, the evolution equations (2)-(7) imply that the Hamiltonian and momentum constraints hold in the form

$$\mathcal{H} \equiv \frac{2}{3}K^2 - \bar{A}_{ij}\bar{A}^{ij} + e^{-4\phi}(\bar{R} - 8\bar{D}^i\phi\bar{D}_i\phi - 8\bar{D}^2\phi) - 16\pi E = 0, \quad (18)$$
$$\mathcal{M}^i \equiv e^{-4\phi}(\frac{1}{\sqrt{\bar{\gamma}}}\hat{D}_j(\sqrt{\bar{\gamma}}\bar{A}^{ij}) + 6\bar{A}^{ij}\partial_j\phi - \frac{2}{3}\bar{\gamma}^{ij}\partial_j K + \bar{A}^{jk}\Delta\Gamma^i_{jk}) - 8\pi S^i = 0, \quad (19)$$

where $\bar{R}$ is the trace of $\bar{R}_{ij}$. We refer to [12] for a complete list of definitions of the variables used here.

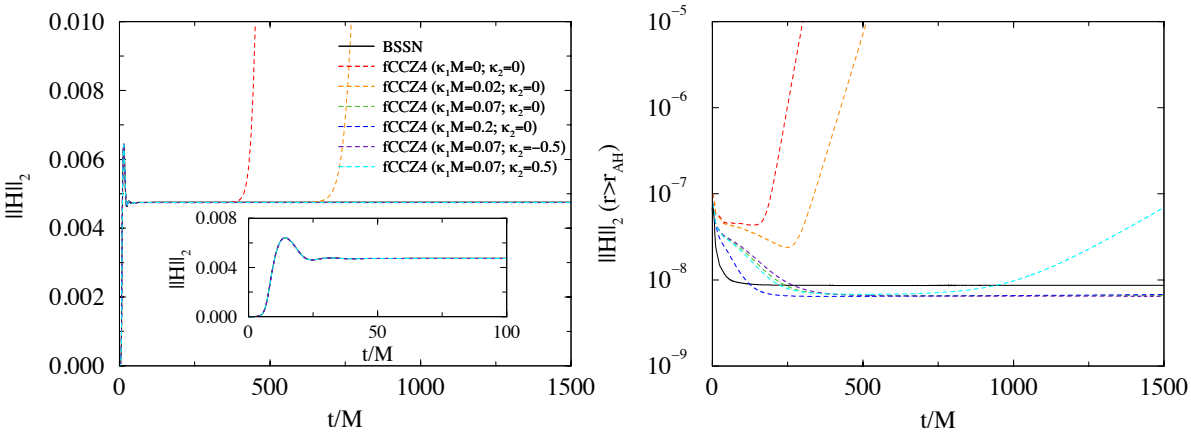


**Figure 1.** *Left panel:* L2-norm of the Hamiltonian constraint in the single puncture black hole simulation. The inset shows a magnified view of the initial $100M$ in the evolution. *Right panel:* Same quantity but computed outside the apparent horizon.

## 3. Numerical Results

The Einstein equations coupled to the general relativistic hydrodynamics equations (see [12] for specific details) are solved using both the BSSN and the fCCZ4 formulations. We show results for two 3D tests, namely the propagation of an axisymmetric Teukolsky wave and the evolution of a rotating neutron star in equilibrium, and only one 1D test, the evolution of a Schwarzschild black hole, addressing the interested reader to [12] for additional tests in the case of spherical symmetry. The 1D test corresponds to spherically symmetric initial data that have been evolved using the 1D code mentioned previously. We note that similar results are found when evolving the same initial data using the 3D code `nada`.

### *3.1. 1D test: Schwarzschild black hole*

We evolve a single Schwarzschild black hole given by wormhole initial data and follow the coordinate evolution to the trumpet geometry. In the left panel of Fig. 1 we plot the L2-norm of the Hamiltonian constraint computed in the whole computational domain (including the interior of the apparent horizon (AH)). The largest violation of the Hamiltonian constraint arises from the finite differencing across the puncture. The right panel of Fig. 1 shows that the L2-norm of the Hamiltonian constraint violation computed outside the AH presents some differences between the two formulations which also depends on the values for the damping coefficients. We observe that the numerical evolutions develop instabilities for $\kappa_2 = 0$ and $\kappa_1 M = (0, 0.02)$. Selecting $\kappa_1 M = 0.07$ and $\kappa_2 = 0.5$ leads to an over-damped behavior that is responsible for an exponential growth of the constraint violation at late times. We find that $\kappa_2 = 0$ with $\kappa_1 M = 0.07$ or $\kappa_1 M = 0.2$ give the best results, leading to constraint violations that are comparable to those achieved with BSSN.

The AH mass is defined as $M_{\rm AH} = \sqrt{A/16\pi}$, where $A$ is the proper area of the horizon. For stable black hole evolutions the difference between the AH mass for BSSN and fCCZ4 is less than 0.005% at the end of the simulation ($t = 1875M$), while the error with respect to the initial ADM mass is $\sim 0.7\%$. We note, however, that the black hole mass continues to drift for the fCCZ4 formulation, while it remains constant after an initial transition for the BSSN formulation.

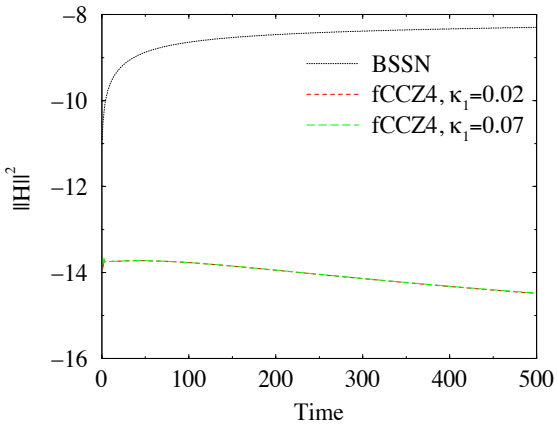


**Figure 2.** Time evolution of the L2 norm of the Hamiltonian constraint of the Teukolsky wave for BSSN and fCCZ4 for different choices of the damping parameter $\kappa_1$, with $\kappa_2 = 0$.

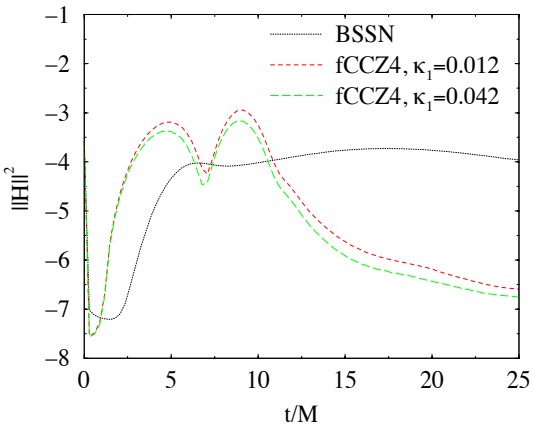


**Figure 3.** Time evolution of the L2 norm of the Hamiltonian constraint of the rotating neutron star for BSSN and fCCZ4 for different choices of the damping parameter $\kappa_1$, with $\kappa_2 = 0$.

*3.2. 3D test: Weak gravitational waves*

As a first 3D test of our fCCZ4 formulation we consider small-amplitude gravitational waves on a flat Minkowski background. We construct an analytical, linear solution for quadrupolar ($l$=2) waves from a function

$$F(r,t) = A(r \mp t)e^{-(r\mp t)^2/\lambda^2} \tag{20}$$

where the constant $A$ is related to the amplitude of the wave and $\lambda$ to its wavelength. For our test we consider the axisymmetric mode $m = 0$, set $\lambda = 1$, and choose an amplitude small enough, $A = 10^{-7}$, to ensure that the test is performed in the linear regime.

In Fig. 2 we show the time evolution of the L2-norm of the Hamiltonian constraint for BSSN and fCCZ4 for two values of the damping parameter $\kappa_1$. In [12] we realized that the influence of the parameter $\kappa_2$ on the results is not important and can even lead to over-damping effects, so we kept $\kappa_2$ equal to zero for most tests. Likewise, we choose $\kappa_2 = 0$ for the present 3D test. Fig. 2 shows that the L2-norm of the Hamiltonian constraint is almost five orders of magnitude smaller for fCCZ4 than for BSSN, as expected. The difference between the two choices of the damping parameter $\kappa_1$ is not noticeable in this case.

*3.3. 3D test: Rotating neutron star*

For our second 3D test we evolve a rapidly rotating relativistic star in equilibrium. The initial data are constructed using the RNS code [15]. In particular, we choose the uniformly rotating BU7 model from [16], a relativistic polytrope with polytropic index $N = 1$ and polytropic constant $K = 100$. This model has a central energy density (in units $G = c = M_\odot = 1$) $\epsilon_c = 1.444 \times 10^{-3}$ and a ratio of polar-to-equatorial coordinate axis $r_p/r_e = 0.65$, resulting in a star with mass $M = 1.666$ and radius $R = 12.3$.

In Fig. 3 we plot the time evolution of the L2-norm of the Hamiltonian constraint for BSSN and fCCZ4 for two different choices of the damping parameter $\kappa_1$ and $\kappa_2 = 0$. Again, when using fCCZ4 we observe a reduction in the violation of the Hamiltonian constraint up to almost

three orders of magnitude with respect to BSSN. Besides, contrary to the previous test, we find that taking a large enough value of $\kappa_1$ leads to slightly smaller constrain violations.

## 4. Summary

The fCCZ4 formulation of the Einstein equations allows us to write the evolution equations in a fully covariant form suitable for curvilinear coordinate systems. In this paper we have discussed the implementation of the fCCZ4 system in spherical coordinates adopting a PIRK scheme for the time evolution. We have shown that this approach leads to stable evolutions – without regularization of the equations at the coordinate singularities – for both vacuum and non-vacuum spacetimes.

We have tested our approach both in a 1D code and in the 3D code `nada`. Our results for non-vacuum spacetimes show that for optimal choices of the constraint damping parameters of fCCZ4, we obtain a reduction from 1 to 3 orders of magnitude of the violations of the Hamiltonian constraint with respect to BSSN. On the other hand, for black hole spacetimes in the spherically symmetric case, we have seen that fCCZ4 offers little advantages over BSSN. We also note, as discussed in detail in [12], that inadequate choices of the damping parameters may lead to over-damping effects. Of both damping parameters, it is $\kappa_1$ the one that plays the most important role in the reduction of the violations of the constraints. Increasing the value of this parameter tends to reduce constraint violations but may also introduce too large damping, thereby making the code unstable and causing it to crash.

The results presented in this work are preliminary. In the near future we plan to fully assess the fCCZ4 formulation in a fully 3D setting by considering more demanding scenarios such as the dynamical evolution of rotating black holes and the gravitational collapse of rotating neutron stars leading to black hole formation, investigating in particular the benefits of the new approach for the extraction of gravitational radiation when employing spherical coordinates.

### *4.1. Acknowledgments*

NSG thanks the Max-Planck-Institut für Astrophysik for its hospitality during the development of part of this project. This work was supported in part by the Spanish MINECO (AYA2013-40979-P), by the Generalitat Valenciana (PROMETEOII-2014-069), by the Deutsche Forschungsgesellschaft (DFG) through its Transregional Center SFB/TR 7 "Gravitational Wave Astronomy", and by NSF grants PHY-1063240 and PHY-1402780 to Bowdoin College.

## 5. References

[1] Bona C., Ledvinka T., Palenzuela C. and Zacek M., Phys. Rev. D **67**, 104005 (2003).
[2] Bernuzzi S. and Hilditch D., Phys. Rev. D **81**, 084003 (2010).
[3] Ruiz M., Hilditch D. and Bernuzzi S., Phys. Rev. D **83**, 024025 (2011).
[4] Weyhausen A., Bernuzzi S. and Hilditch D., Phys. Rev. D **85**, 024038 (2012).
[5] Hilditch D., Bernuzzi S., Thierfelder M., Cao Z., Tichy W. and Brügmann B., Phys. Rev. D **88**, 084057 (2013).
[6] Alic D., Bona-Casas C., Bona C., Rezzolla L., and Palenzuela C., Phys. Rev. D **85**, 064040 (2012).
[7] Alic D., Kastaun W. and Rezzolla L., Phys. Rev. D **88**, 064049 (2013).
[8] Gundlach C., Martin-Garcia J. M., Calabrese G. and Hinder I., Classical Quantum Gravity **22**, 3767 (2005).
[9] Nakamura T., Oohara K. and Kojima Y., Prog. Theor. Phys. Suppl. **90**, 1 (1987).
[10] Shibata M. and Nakamura T., Phys. Rev. D **52**, 5428 (1995).
[11] Baumgarte T. W. and Shapiro S. L., Phys. Rev. D **59**, 024007 (1998).
[12] Sanchis-Gual N., Montero P. J., Font J. A., Müller E. and Baumgarte T. W. Phys. Rev. D **89**, 104033 (2014).
[13] Baumgarte T. W., Montero P. J., Cordero-Carrión I. and Müller E., Phys. Rev. D **87**, 044026 (2013).
[14] Montero P. J., Baumgarte T. W. and Müller E., Phys. Rev. D **89**, 084043 (2014).
[15] Stergioulas N. and Friedman J. L., ApJ, **444**, 306, (1995).
[16] Dimmelmeier H., Stergioulas N. and Font J. A., Mon. Not. R. Astron. Soc. **368**, 1609-1630, (2006).